PERGAMON

International Journal of Heat and Mass Transfer 45 (2002) 5025–5034

International Journal of HEAT and MASS TRANSFER

www.elsevier.com/locate/ijhmt

An experimental investigation of convection heat transfer to supercritical carbon dioxide in miniature tubes

S.M. Liao, T.S. Zhao *

Department of Mechanical Engineering, The Hong Kong University of Science and Technology, Clear Water Bay, Kowloon, Hong Kong, China

Received 22 December 2001; received in revised form 8 May 2002

Abstract

Experimental results of convection heat transfer to supercritical carbon dioxide in heated horizontal and vertical miniature tubes are reported in this paper. Stainless steel circular tubes having diameters of 0.70, 1.40, and 2.16 mm were investigated for pressures ranging from 74 to 120 bar, temperatures from 20 to 110 °C, and mass flow rates from 0.02 to 0.2 kg/min. The corresponding Reynolds numbers and Prandtl numbers ranged from 10^4 to 2×10^5 and from 0.9 to 10, respectively. It is found that the buoyancy effects were significant for all the flow orientations, although Reynolds numbers were as high as 10^5. The experimental results reveal that in downward flow, a significant impairment of heat transfer was discerned in the pseudocritical region, although heat transfer for both horizontal and upward flow was enhanced. The experimental results further indicate that in all the flow orientations, the Nusselt numbers decreased substantially as the tube diameter shrunk to <1.0 mm. Based on the experimental data, correlations were developed for the axially-averaged Nusselt number of convection heat transfer to supercritical carbon dioxide in both horizontal and vertical miniature heated tubes.

Keywords: Supercritical carbon dioxide; Heat transfer; Miniature tubes

1. Introduction

Heat transfer to supercritical fluids near their critical points is important in a number of technological applications. In modern power plants, heat is transferred to supercritical water. Superconductivity effects are achieved by cooling the conductor with fluids that are close to their critical points. Rockets and military aircraft are cooled using fuel at supercritical pressure as an onboard coolant. Highly charged machine elements such as gas turbine blades, supercomputer elements, magnets and power transmission cables are cooled with supercritical fluids.

One of the most important characteristics of supercritical fluids near their critical points is that their physical properties exhibit extremely rapid variations with a change in temperature, especially near the pseudocritical point (the temperature at which the specific heat reaches a peak for a given pressure).

Forced convection of supercritical fluids such as water, carbon dioxide, nitrogen, hydrogen, and helium in large channels has been extensively studied both experimentally [1–3] and numerically [4–6]. Many correlations, most of the Dittus–Boelter type ($Nu = CRe^m Pr^n$), have been proposed for supercritical fluids with heating. The reference-temperature method and the property-ratio method have been employed to incorporate the variable-property effect [7]. Comprehensive reviews on previous works associated with variable-property heat transfer and supercritical heat transfer are given by Kakac [7], Hall [8], and Polyakov [9]. It is generally agreed that the correlations do not show sufficient agreement with experiments to justify their use except in very limited conditions. The limitations imposed on a specific correlation should be carefully studied before its

* Corresponding author. Tel.: +852-2358-8647; fax: +852-2358-1543.

E-mail address: metzhao@ust.hk (T.S. Zhao).

0017-9310/02/$ - see front matter
PII: S0017-9310(02)00206-5

Nomenclature

A	inner surface of the test tube, m^2
c_p	specific heat, J/K kg
d	inside-diameter of the test tube, m
g	acceleration of gravity, m/s^2
Gr	Grashof number, $Gr = ((\rho_b - \rho_w)\rho_b g d^3)/\mu_b^2$
Gr_m	Grashof number, $Gr_m = ((\rho_b - \rho_m)\rho_b g d^3)/\mu_b^2$
h	average heat transfer coefficient, W/m^2 K
i	enthalpy, J/kg
k	thermal conductivity, W/m K
LMTD	logarithmic mean temperature difference, °C
$\dot{m}$	mass flow rate, kg/s
Nu	Nusselt number
p	pressure, bar
Pr	Prandtl number
$\dot{Q}$	heat transfer rate, W
q''	heat flux, W/m^2
Re	Reynolds number
T	temperature, °C or K

Greek symbols

μ	dynamic viscosity, kg/m s
ν	kinematic viscosity, m^2/s
ρ	density, kg/m^3
ρ_m	integrated density, $\rho_m = \frac{1}{T_w - T_b}\int_{T_b}^{T_w} \rho \, dT$, kg/m^3

Subscripts

b	bulk fluid
cr	critical
db	Dittus–Boelter correlation
in	CO_2 inlet of the test section
out	CO_2 exit of the test section
pc	pseudocritical
w	wall

use in practical applications. Most recently, to meet the demand for designs of gas coolers in transcritical CO_2 refrigeration systems, a few papers [10,11] have reported on the study of heat transfer of supercritical CO_2 flowing in mini/microchannels under cooling conditions.

The purpose of this study was to study the heat transfer of supercritical CO_2 flowing in miniature circular tubes under heating conditions. Three circular tubes having inside-diameters of 0.70, 1.40, and 2.16 mm were tested. Measurements were carried out at pressures ranging from 74 to 120 bar and temperatures ranging from 20 to 110 °C. The critical pressure and the critical temperature of CO_2 are $p_{cr} = 73.8$ bar and $T_{cr} = 31.1$ °C, respectively. In the following, we first describe our experimental apparatus and procedures. We then report the experimental results to show the effect of some important parameters including pressure, flow orientation, tube diameter, and heat flux on heat transfer behavior. Finally, the salient findings of the study are summarized.

2. Experimental apparatus and procedures

The test loop, schematically shown in Fig. 1, is essentially the same as that used for studying heat transfer of supercritical CO_2 under cooling conditions [11]. It consisted of a compressed CO_2 cylinder, a high-pressure CO_2 pump, a filter, a flow meter, a pre-heater, a test section, an after-cooler, and a number of high-pressure fittings and valves. CO_2 with a purity of 99.5% was fed to the test loop from the compressed CO_2 cylinder and was circulated by the CO_2 pump (Model P-200, Thar Designs), with an input pressure of 57 bar, a discharge pressure up to 680 bar, and a maximum mass flow rate

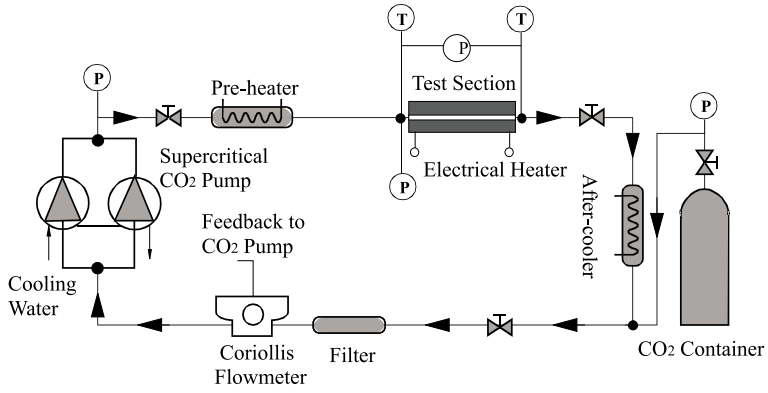

Fig. 1. Schematic diagram of the experimental apparatus.

of 0.2 kg/min. The pump is controllable based on feedback from a pressure sensor or a flow meter. The mass flow rate was measured using a Coriolis-type Micro Motion mass flow meter (Model CFM-010M, with IFT9701 transmitter). The nominal range of the flow meter is 0–1.37 kg/min (0–22.8 g/s), with an accuracy of $< \pm 0.2\%$ of the reading. A pressure gage transducer (Model 3051CG5, Rosemount) was used to measure the static pressure at the inlet of the test section, while a differential pressure transducer (Model 3051CD3, Rosemount) was installed at both ends of the test section to measure the pressure drops. The pressure gage transducer and the differential pressure transducer were calibrated using a pressure calibrator, and the accuracy of the transducers was found to be $\pm 0.2\%$ of the reading. The onboard microprocessor monitored the flow meter, calculated the flow rate and sent the feedback to the pump. In addition, a portable chiller was used to provide cooling for the CO_2 pump and the after-cooler.

Three circular tubes (stainless steel AISI 304) having inside/outside-diameters of 0.70 mm/1.10 mm, 1.40 mm/3.18 mm, and 2.16 mm/3.18 mm were tested. Fig. 2 shows the details of the test section. The test tube was inserted tightly into a copper cylinder having an outsider-diameter of 25 mm and a length of 110 mm. An electrical resistance wire wrapped around the cylindrical copper was used to heat the test tube and was electrically insulated from the cylindrical copper with isinglass and thermally insulated from the ambient air with fiber glass wool. A thermally insulated length of 110.0 mm preceded the heated length of 110.0 mm, which was followed by a thermally insulated exit length of 40.0 mm. Between the test tube and the cylindrical copper, a thin layer of a metal oxide filled silicone oil paste (Heat Sink Compound Plus, RS) was laid to reduce the contact thermal resistance, and six uniformly spaced T-type thermocouples were placed there to measure the outer surface temperatures of the test tube. The temperatures of the CO_2 at both the inlet (T_{in}) and the outlet (T_{out}) of the test tube were measured by two armored T-type thermocouples. All the thermocouples were calibrated in a constant temperature bath and the measurement error was found to be within ± 0.2 °C. The temperature of the CO_2 at the inlet of the test tube was regulated by the preheater.

The heat transfer rate, $\dot{Q}$, from the tube wall to the CO_2 can be obtained from the energy balance under a steady state:

$$\dot{Q} = \dot{m}(i_{out} - i_{in}), \tag{1}$$

where $\dot{m}$ is the mass flow rate, and i_{in} and i_{out} denote the enthalpy of the CO_2 at the inlet and the outlet of the test section, respectively. The test data of the heat transfer rate $\dot{Q}$ obtained from Eq. (1) were compared with the test data of the electrical heating power of the heater outside the test tube. The electrical heating power was obtained by measuring the voltages and the currents of the heater. The differences between the heat transfer rate and the electrical heating power were within 12% for all the test data.

Since the addition of heat to the test tube was accomplished by heating the outer copper cylinder, which enhanced the axial heat conduction, the boundary condition for the test tubes was close to a constant temperature condition rather than to a constant heat flux condition [12]. The outer wall mean temperature averaged over the entire heated length was obtained based on the readings of the six thermocouples under each test condition. A corresponding inner wall mean temperature of the test section T_w can then be calculated based on the wall thickness of the test tube, the outer wall mean temperature and the heating power given by Eq. (1). Subsequently, the logarithmic mean temperature difference LMTD can be obtained for the test tube as:

$$\mathrm{LMTD} = \frac{(T_w - T_{in}) - (T_w - T_{out})}{\ln \frac{T_w - T_{in}}{T_w - T_{out}}}. \tag{2}$$

Note that in all the experiments, for a given addition of heat to the test section, the temperature change in the CO_2 ($T_{out} - T_{in}$) near the pseudocritical point was usually very small (<2 °C) because the specific heat over this range was very high. On the other hand, large temperature changes (about 12° C) in the CO_2 took place far

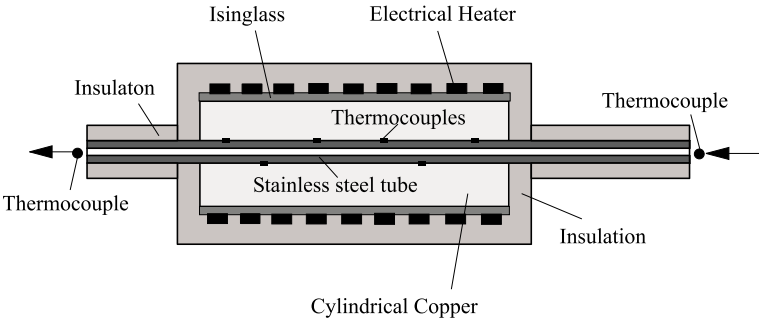

Fig. 2. Schematic diagram of the test section.

from the pseudocritical point and the specific heat was nearly constant over this temperature range. This means that the use of the LMTD in this study can be justified.

The average heat transfer coefficient h over the entire heated length is determined from

$$h = \frac{\dot{Q}}{A\,\mathrm{LMTD}}, \tag{3}$$

where A represents the inner surface of the test tube. The Nusselt number is defined as

$$Nu_{\mathrm{b}} = \frac{hd}{k_{\mathrm{b}}}, \tag{4}$$

where d is the tube diameter, k is the thermal conductivity of CO_2, and the subscript b represent the case in which the properties are evaluated at the bulk CO_2 mean temperature T_{b} defined as:

$$T_{\mathrm{b}} = \frac{T_{\mathrm{in}} + T_{\mathrm{out}}}{2}, \tag{5}$$

with T_{in} and T_{out} being the CO_2 temperature at the inlet and the outlet of the test section.

All the experimental data reported in this paper were processed based on the data for the physical properties of CO_2 provided by the NIST Refrigerants Database (REFPROP) [13]. The uncertainties in the experimental data were evaluated according to the methods introduced in NIST Technical Note 1297 [14]. Since near the pseudocritical temperature T_{pc}, the thermal properties become rather sensitive to temperature (see Fig. 1), a small error in temperature measurements will cause a large uncertainty in the Nusselt numbers. For this reason, the uncertainty of the Nusselt number Nu_{b} near the pseudocritical temperature ($T_{\mathrm{pc}} \pm 3$°C) could be up to 30%. Except for the measuring points near the pseudocritical temperature, it is estimated that the relative standard uncertainty of the Nusselt numbers Nu_{b} and Nu_{w} was within 8%.

3. Results and discussion

Measurements were carried out at CO_2 pressures ranging from 74 to 120 bar, temperatures from 20 to 110 °C, and mass flow rates from 0.02 to 0.2 kg/min. Resulting temperature differences ($T_{\mathrm{b}} - T_{\mathrm{w}}$) between the bulk CO_2 and the wall ranged from 2 to 30 °C, and heat fluxes ranged from 10^4 to 2×10^5 W/m^2. The corresponding Reynolds numbers Re_{b} and Prandtl numbers Pr_{b} ranged from 10^4 to 2×10^5 and from 0.9 to 10, respectively.

3.1. General behavior

Fig. 3 shows the variation in the heat transfer coefficient h with the bulk mean temperature of CO_2 for the horizontal tube of $d = 1.40$ mm for the mass flow rate of $\dot{m} = 0.050$ kg/min at static pressures of $p = 80$ and 100 bar. It is seen that there was a peak of the heat transfer coefficient for each pressure near the corresponding pseudocritical temperature ($T_{\mathrm{pc}} = 34.6$ °C at $p = 80$ bar and $T_{\mathrm{pc}} = 45.0$ °C at $p = 100$ bar), indicating that heat transfer was enhanced near the pseudocritical region in horizontal tubes. The behavior of the heat transfer coefficient in the vicinity of the pseudocritical temperature is mainly attributed to the fact that the specific heat c_p varies in a similar manner near the pseudocritical region. Fig. 3 also indicates that the peak value of the heat transfer coefficient decreased as the static pressure was increased from 80 to 100 bar. This is because the peak value of the specific heat c_p decreases with an increase in pressure.

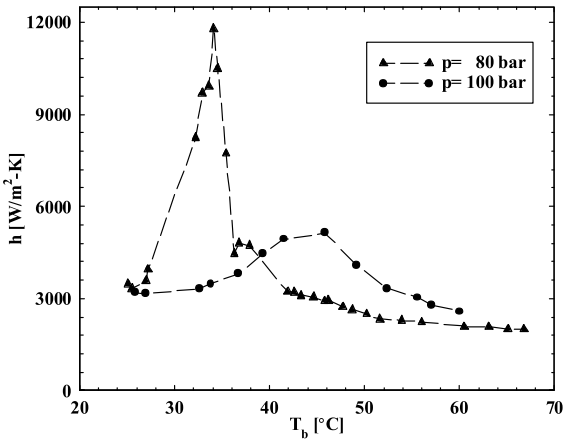

Fig. 3. Variations in the heat transfer coefficient h with the bulk mean temperature for the horizontal tube of $d = 1.40$ mm at $\dot{m} = 0.05$ kg/min and static pressures of 80 and 100 bar.

The variations in the heat transfer coefficient h with the bulk mean temperature for the tube of $d = 0.70$ mm for $\dot{m} = 0.050$ kg/min at $p = 80$ bar are compared in Fig. 4 for different flow orientations. It is evident from this figure that near the pseudocritical temperature ($T_{\mathrm{pc}} =$ 34.6°C), heat transfer in both horizontal and upward flow was enhanced tremendously, reflected by the high peak values when the bulk temperature passed through T_{pc}. However, it is also clear from Fig. 4 that in downward flow, the heat transfer coefficient decreased significantly near the pseudocritical region. It can also be observed that, in the region where the bulk mean temperature was higher than the pseudocritical point the heat transfer coefficients for downward flow were generally lower than those for horizontal and upward flow. Similar behavior of the heat transfer coefficient can be observed in Fig. 5 for the tube of $d = 1.40$ mm for $\dot{m} = 0.100$ kg/min at $p = 80$ bar and in Fig. 6 for the tube of $d = 2.16$ mm for $\dot{m} = 0.154$ kg/min at $p = 80$

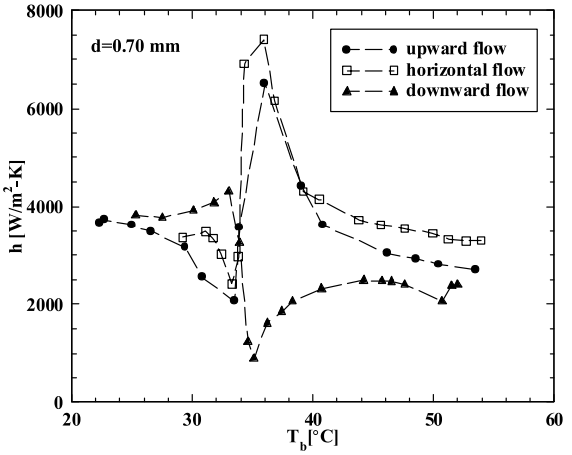

Fig. 4. Variations in the heat transfer coefficient h with the bulk mean temperature for the tube of $d = 0.70$ mm at $\dot{m} = 0.05$ kg/min in horizontal, upward, and downward flow.

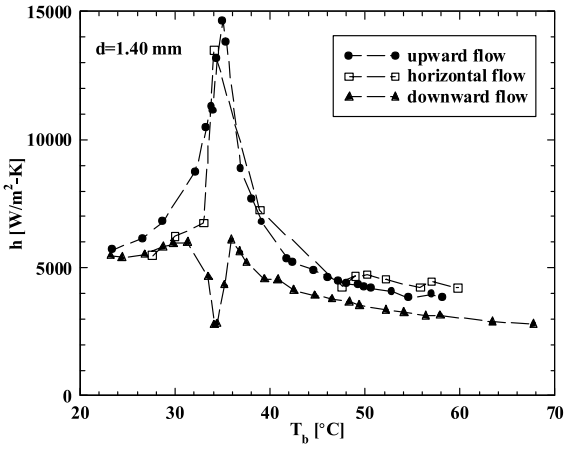

Fig. 5. Variations in the heat transfer coefficient h with the bulk mean temperature for the tube of $d = 1.40$ mm at $\dot{m} = 0.100$ kg/min in horizontal, upward, and downward flow.

bar. The different heat transfer behaviors caused by the change in flow orientations suggest that the buoyancy effect was still significant for heat transfer of supercritical CO_2 flowing in the tube having a diameter as small as 0.70 mm and at Reynolds numbers up to 10^5. Previous investigations on mixed turbulent convection in large tubes showed that buoyancy always enhanced the heat transfer in downward flow (buoyancy-opposed flow), whereas it might impair or enhance heat transfer in upward flow (buoyancy-aided flow), depending on the strength of the free convection [15,16]. The results presented in Figs. 4–6 indicate that, due to buoyancy effects, the heat transfer coefficients for downward flow in miniature tubes decreased significantly. Apparently, the present experimental results did not support the conclusions reached in the previous investigations on mixed turbulent convection in large vertical tubes. Instead, the present experimental results suggest that the heat transfer behaviors for turbulent convection in miniature vertical tubes under some conditions are in agreement with the theory of laminar mixed convection in vertical tubes [16].

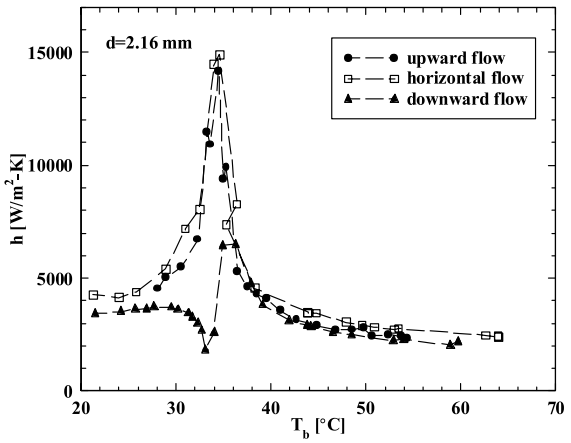

Fig. 6. Variations in the heat transfer coefficient h with the bulk mean temperature for the tube of $d = 2.16$ mm at $\dot{m} = 0.154$ kg/min in horizontal, upward, and downward flow.

Fig. 7 shows the effect of the tube diameter on the Nusselt number Nu_b for horizontal flow at $p = 80$ bar. To create meaningful comparisons, the experiments were conducted at a fixed ratio of the mass flow rate to the tube diameter ($\dot{m}/d = 1.19$ kg/m s) in order to keep both the Reynolds number Re_b and the Prandtl number Pr_b constant in the three tubes of different diameters ($d = 0.70$, 1.40, and 2.16 mm) at a given bulk mean

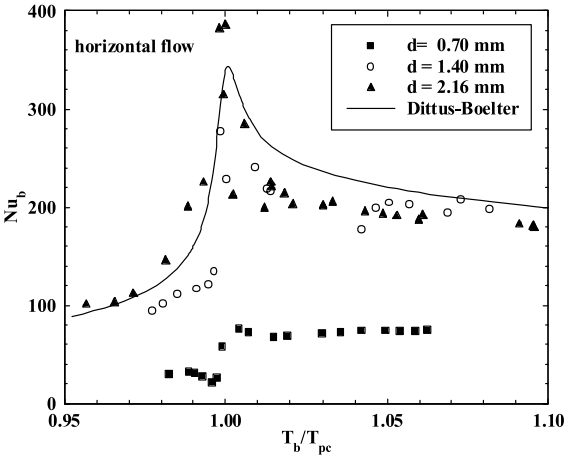

Fig. 7. Effects of tube diameter on the Nusselt number Nu_b at $\dot{m}/d = 1.19$ kg/m s and $p = 80$ bar in horizontal flow.

temperature of the fluid. In the above-described experimental conditions, the Reynolds number Re_b ranged from 2×10^4 to 8×10^4 and the Prandtl number Pr_b ranged from 0.9 to 10 as the bulk mean temperature of the fluid changed. The abscissa in the figure is the dimensionless bulk mean temperature T_b/T_{pc}, where T_{pc} represents the pseudocritical temperature of CO_2. Note that the unit of temperature is K in calculating the ratio T_b/T_{pc}. For comparison, the Dittus–Boelter correlation for heating constant property fluids

$$Nu_b = 0.023 Re_b^{0.8} Pr_b^{0.4}, \tag{6}$$

is also plotted in Fig. 7. It is noted from Fig. 7 that the experimental measurements for the tube of $d = 0.70$ mm were only 15–35% of the values predicted by Eq. (6), although most of the experimental data for the tubes of $d = 2.16$ and 1.40 mm were favorably in agreement with Eq. (6). The Nusselt numbers for supercritical CO_2 in the range of the measured temperatures ($0.95 < T_b/T_{pc} < 1.10$) depended very much on the tube diameter, and they dropped substantially as the tube diameter was reduced from 2.16 to 0.70 mm. Fig. 8 presents similar results for upward flow. It is seen from Fig. 8 that the experimental data for the tubes of $d = 2.16$ and 1.40 mm were close to the prediction by Eq. (6) when $T_b/T_{pc} < 0.995$, whereas the experimental data deviated substantially from the prediction by Eq. (6) when $T_b/T_{pc} > 0.995$. The experimental data for the tube of $d = 0.70$ mm were only 15–30% of the values predicted by Eq. (6). It can also be seen in Fig. 8 that the Nusselt numbers dropped substantially as the tube diameter was reduced from 2.16 to 0.70 mm. Similar results for downward flow are presented in Fig. 9. It is seen from Fig. 9 that the experimental data for the three tubes were lower than the values predicted by Eq. (6). Again, the

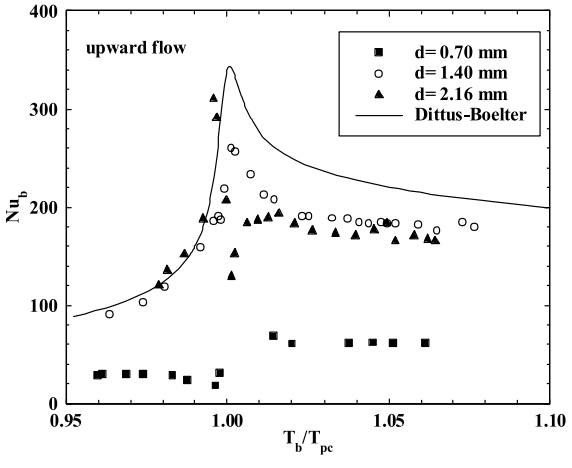

Fig. 8. Effects of tube diameter on the Nusselt number Nu_b at $\dot{m}/d = 1.19$ kg/m s and $p = 80$ bar in upward flow.

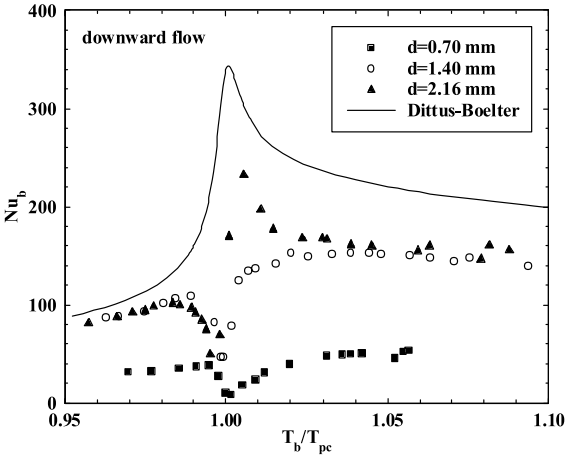

Fig. 9. Effects of tube diameter on the Nusselt number Nu_b at $\dot{m}/d = 1.19$ kg/m s and $p = 80$ bar in downward flow.

Nusselt number dropped substantially as the tube diameter was reduced from 2.16 to 0.70 mm. One of the major reasons for the above-described heat transfer behaviors in relation to changes in tube sizes might be from the buoyancy effect.

For horizontal tubes, it has been shown theoretically that when

$$\frac{Gr}{Re_b^2} < 10^{-3}, \tag{7}$$

the effect of the buoyancy-induced secondary flow becomes negligible [7,17], where the Grasholf number Gr is defined as:

$$Gr = \frac{(\rho_w - \rho_b) g d^3}{\rho_b \nu_b^2} = \frac{(\rho_w - \rho_b)\rho_b g d^3}{\mu_b^2}, \tag{8}$$

with ρ_b and ρ_w denoting the density of CO_2 evaluated at the bulk mean temperature T_b and the wall mean temperature T_w, respectively; ν_b and μ_b represent the kinetic viscosity and dynamic viscosity of CO_2 evaluated at the bulk mean temperature T_b, respectively; and g is the acceleration of gravity.

Let us now examine the range of Gr/Re_b^2 for the measured Nusselt numbers Nu_b presented in Fig. 7. As noted from Fig. 10, Gr/Re_b^2 for the tubes of $d = 2.16$ and 1.40 mm was higher than 10^{-3} (see Eq. (7)) when $T_b/T_{pc} < 1.01$, but it was lower than 10^{-3} when $T_b/T_{pc} > 1.01$, meaning that buoyancy effects are important at low temperatures ($T_b/T_{pc} < 1.01$), but they become less important at high temperatures ($T_b/T_{pc} > 1.01$). However, it is clear from Fig. 10 that for the tube of $d = 0.70$ mm, Gr/Re_b^2 was lower than 10^{-3} over the entire temperature range, indicating that the buoyancy effect is less important for this small tube. It is also seen from Fig. 10 that Gr/Re_b^2 grew smaller as the tube diameter was decreased.

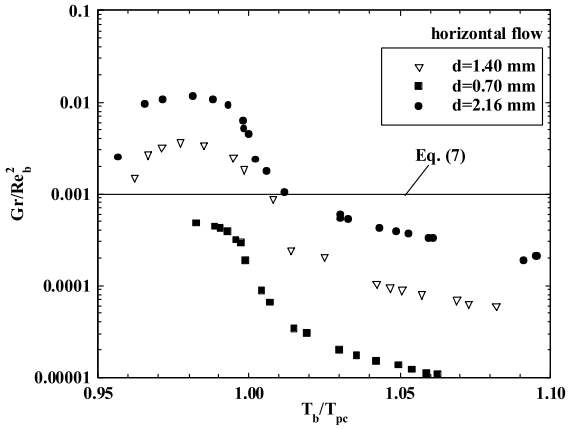

Fig. 10. Gr/Re_b^2 values vs. T_b/T_{pc} at $\dot{m}/d = 1.19$ kg/m s for the horizontal tubes.

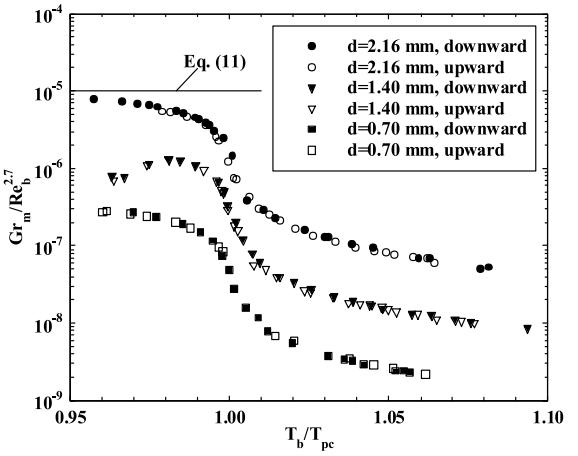

Fig. 11. $Gr_m/Re_b^{2.7}$ values vs. T_b/T_{pc} at $\dot{m}/d = 1.19$ kg/m s for the vertical tubes.

Considering that the buoyancy parameter Gr/Re_b^2 is proportional to the tube diameter d, it can be concluded that the reduction in the Nusselt number because of reduction in the tube size was caused, partly at least, by the fact that the buoyancy effect became less important in small tubes.

For vertical tubes, the influences of buoyancy on heat transfer behaviors are more complex. Previous investigations on turbulent mixed convection in a large heated tube showed that heat transfer was always enhanced by buoyancy in downward flow (buoyancy-opposed flow under the heating condition) [15,16]. However, in upward flow (buoyancy-aided flow) heat transfer might be enhanced or impaired, depending on the strength of free convection. Moreover, it has been shown that the influences of buoyancy were controlled by the magnitude of the Grashof number and the Reynolds number in the form Gr_m/Re_b^2, where Gr_m is defined as

$$Gr_m = \frac{(\rho_b - \rho_m)gd^3}{\rho_b \nu_b^2} = \frac{(\rho_b - \rho_m)\rho_b g d^3}{\mu_b^2}, \tag{9}$$

with the integral density ρ_m being given by

$$\rho_m = \frac{1}{T_w - T_b}\int_{T_b}^{T_w} \rho \, dT. \tag{10}$$

An approximate analysis [15] indicated that buoyancy-induced impairment of heat transfer in upward flow could be ignored when

$$\frac{Gr_m}{Re_b^{2.7}} < 10^{-5}. \tag{11}$$

We now use Eq. (11) to examine our experimental results. To this end, the range of $Gr_m/Re_b^{2.7}$, over which the experimental data shown in Figs. 8 and 9 were collected for the vertical tubes of $d = 0.70$, 1.40, and 2.16 mm, was plotted against the range of T_b/T_{pc} in Fig. 11. Note that the heat transfer coefficients h for vertical tubes presented in Figs. 4–6 were also measured at the same range of $Gr_m/Re_b^{2.7}$ as illustrated in Fig. 11. It is noted from Fig. 11 that all the values of the parameter $Gr_m/Re_b^{2.7}$, no matter in upward and downward flow, were lower than 10^{-5}. The results presented in Figs. 4–6 in upward flow did not show significant heat transfer impairment, implying that Eq. (11) is consistent with the present results in upward flow. It should be recognized that although all the values of the parameter $Gr_m/Re_b^{2.7}$ were lower than 10^{-5}, buoyancy effects on heat transfer were still significant, reflected by the fact that there was a significant difference of the heat transfer coefficients between upward flow and downward flow as shown in Figs. 4–6. This is true even for very small values of $Gr_m/Re_b^{2.7}$ ranging from 2×10^{-9} to 5×10^{-7} for the smallest tube ($d = 0.70$ mm). On the other hand, the experimental data in downward flow in this study have shown that heat transfer was impaired in all the tested tubes. This behavior is inconsistent with the previous work [15,16] for turbulent mixed convection in large vertical tubes, in which heat transfer in downward flow was found to be enhanced by buoyancy.

The criterion for negligible heat transfer impairment given by Eq. (11) can be further discussed by referring to Fig. 12, where the measured Nu_b in upward flow in the tube of $d = 2.16$ mm at $\dot{m} = 0.050$ kg/min, together with the range of $Gr_m/Re_b^{2.7}$, were plotted against T_b/T_{pc}. For comparison, the Nusselt number Nu_{db} predicted by the Dittus–Boelter correlation (Eq. (6)) for constant property fluids was also plotted in Fig. 12. It is seen that when $Gr_m/Re_b^{2.7} > 10^{-5}$ ($T_b/T_{pc} < 1$) the measured Nu_b was much lower than that predicted by the Dittus–Boelter correlation. This observation suggests that the buoyancy-induced impairment of heat transfer cannot be neglected in upward flow, which agrees with Eq. (11).

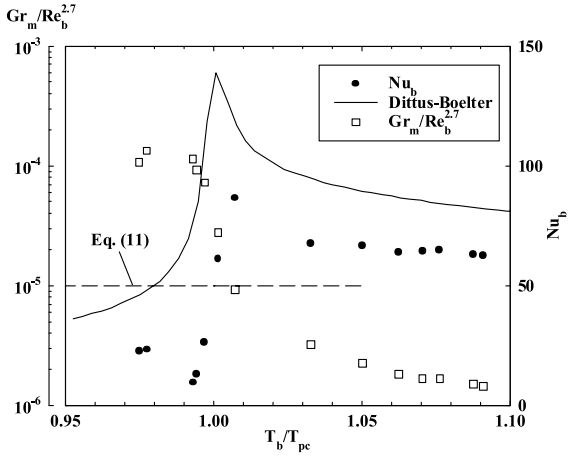

Fig. 12. $Gr_m/Re_b^{2.7}$ and Nu_b values vs. T_b/T_{pc} at $d = 2.16$ mm and $\dot{m} = 0.050$ kg/min in upward flow.

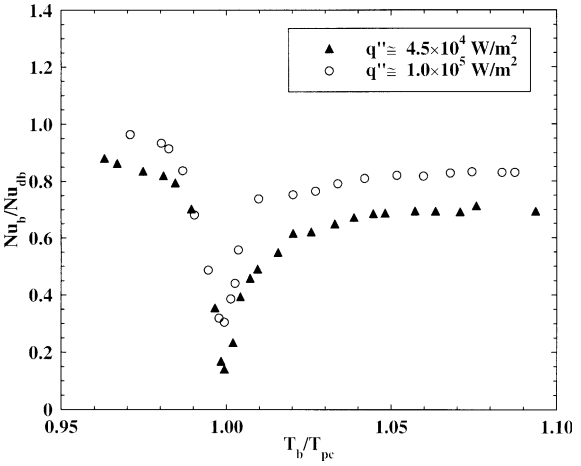

Fig. 13. Effects of the heat flux on the Nusselt number Nu_b for $d = 1.40$ mm at $\dot{m} = 0.100$ kg/min and $p = 80$ bar in downward flow.

As buoyancy effects on heat transfer for vertical tubes are controlled by $Gr_m/Re_b^{2.7}$ and this parameter is proportional to $d^{0.3}$, buoyancy should be one of the major reasons for the size effect on Nusselt numbers in vertical tubes as shown in Figs. 8 and 9. However, our experimental results show that the Nusselt numbers in both upward flow and downward flow reduced significantly as tube diameter was decreased. For this reason, there might be some other physical mechanisms leading to smaller Nusselt numbers for vertical tubes, in addition to the buoyancy effect.

In order to examine the effect of the heat flux on the heat transfer performance, the reduced Nusselt number Nu_b/Nu_{db} under two different values of the heat flux ($q'' = 4.5 \times 10^4$ and 1.0×10^5 W/m^2) for $d = 1.40$ mm at $\dot{m} = 0.100$ kg/min and $p = 80$ bar in downward flow were compared in Fig. 13. The experimental results indicate that the reduced Nusselt numbers changed significantly as the heat flux changed even if other conditions remained the same, implying that the heat flux has an important influence on the heat transfer rate for supercritical fluids. This is because different heat fluxes will give different velocity and temperature profiles. The change in heat flux corresponds to the change in the temperature difference $(T_w - T_b)$ between the wall mean and the bulk mean temperature. Fig. 13 also shows that the heat transfer performance of supercritical CO_2 in downward flow was impaired significantly ($Nu_b/Nu_{db} \ll 1$) near the pseudocritical point ($T_b/T_{pc} \cong 1$) compared to that of constant property fluids. In developing heat transfer correlations, the influence of the heat flux or the influence of the temperature difference $(T_w - T_b)$ between the bulk mean and wall mean temperature on the heat transfer rate are usually taken into account by using appropriate property parameter groups such as ρ_b/ρ_w, $\bar{c}_p/c_{p,b}$, etc. The mean specific heat $\bar{c}_p$ is defined as:

$$\bar{c}_p = \frac{i_w - i_b}{T_w - T_b}, \tag{12}$$

where i_b and i_w denote the enthalpy of CO_2 evaluated at the bulk mean temperature T_b and the wall mean temperature T_w, respectively.

3.2. Heat transfer correlations

Our experimental results suggest that both the buoyancy effect and the heat flux or the temperature difference between the bulk fluid and the wall must be taken into account in developing heat transfer correlations for heat transfer to supercritical CO_2 flowing through miniature tubes. As seen from the following paragraphs, buoyancy effects on heat transfer in horizontal and vertical tube flow are accounted for by the parameters Gr/Re_b^2 and $Gr_m/Re_b^{2.7}$, respectively. Since Gr/Re_b^2 and $Gr_m/Re_b^{2.7}$ are proportional, respectively, to tube diameter d and $d^{0.3}$ all the effects due to the change of tube diameter are implicitly included in the heat transfer correlations.

In horizontal flow, the following correlation was obtained for convection of supercritical CO_2 in miniature tubes heated at an approximate constant temperature based on a least square fit of 68 experimental data for the circular tubes of $d = 0.70$, 1.40, and 2.16 mm:

$$\frac{Nu_b}{Nu_{db}} = 5.37\left(\frac{Gr}{Re_b^2}\right)^{0.203}\left(\frac{\rho_w}{\rho_b}\right)^{0.842}\left(\frac{\bar{c}_p}{c_{p,b}}\right)^{0.384}. \tag{13}$$

Substituting Eq. (6) into Eq. (13) yields:

$$Nu_b = 0.124 Re_b^{0.8} Pr_b^{0.4} \left(\frac{Gr}{Re_b^2}\right)^{0.203} \left(\frac{\rho_w}{\rho_b}\right)^{0.842} \left(\frac{\bar{c}_p}{c_{p,b}}\right)^{0.384}. \quad (14)$$

The maximum relative error between Eq. (14) and the experimental data is about 21.8%, while the mean relative error between Eq. (14) and the experimental data is about 13.5%.

In upward flow, a least square fit of 66 experimental data for the circular tubes of $d = 0.70$, 1.40, and 2.16 mm heated at an approximate constant temperature yields the following correlation:

$$\frac{Nu_b}{Nu_{db}} = 15.37 \left(\frac{Gr_m}{Re_b^{2.7}}\right)^{0.157} \left(\frac{\rho_w}{\rho_b}\right)^{1.297} \left(\frac{\bar{c}_p}{c_{p,b}}\right)^{0.296} \quad (15)$$

or

$$Nu_b = 0.354 Re_b^{0.8} Pr_b^{0.4} \left(\frac{Gr_m}{Re_b^{2.7}}\right)^{0.157} \left(\frac{\rho_w}{\rho_b}\right)^{1.297} \left(\frac{\bar{c}_p}{c_{p,b}}\right)^{0.296}. \quad (16)$$

The maximum relative error between Eq. (16) and the experimental data is about 18.6%, while the mean relative error between Eq. (16) and the experimental data is about 12.3%.

In downward flow, a least square fit of 70 experimental data for the circular tubes of $d = 0.70$, 1.40, and 2.16 mm heated at an approximate constant temperature leads to the correlation equations as follows:

$$\frac{Nu_b}{Nu_{db}} = 27.94 \left(\frac{Gr_m}{Re_b^{2.7}}\right)^{0.186} \left(\frac{\rho_w}{\rho_b}\right)^{2.154} \left(\frac{\bar{c}_p}{c_{p,b}}\right)^{0.751} \quad (17)$$

or

$$Nu_b = 0.643 Re_b^{0.8} Pr_b^{0.4} \left(\frac{Gr_m}{Re_b^{2.7}}\right)^{0.186} \left(\frac{\rho_w}{\rho_b}\right)^{2.154} \left(\frac{\bar{c}_p}{c_{p,b}}\right)^{0.751}. \quad (18)$$

The maximum relative error between Eq. (18) and the experimental data is about 22.4%, while the mean relative error between Eq. (18) and the experimental data is about 15.6%.

Eqs. (14), (16), and (18) are valid for long tubes of $0.70 \leqslant d \leqslant 2.16$ mm in the range of $74 \leqslant p \leqslant 120$ bar, $20 \leqslant T_b \leqslant 110$ °C, $2 \leqslant T_w - T_b \leqslant 30$ °C, $0.02 \leqslant \dot{m} \leqslant 0.2$ kg/min. In addition, Eq. (14) is valid for the range of $10^{-5} \leqslant Gr/Re_b^2 \leqslant 10^{-2}$, while Eqs. (16) and (18) are valid for the range of $2 \times 10^{-9} \leqslant Gr_m/Re_b^{2.7} \leqslant 10^{-5}$.

4. Concluding remarks

Experimental data on heat transfer to supercritical carbon dioxide flowing in horizontal and vertical miniature circular tubes having inside-diameter of 0.70, 1.40, and 2.16 mm have been presented. The experiments were undertaken under CO_2 pressures ranging from 74 to 120 bar and temperatures ranging from 20 to 110 °C. It has been shown that although supercritical CO_2 was in forced motion at Reynolds numbers up to 10^5, the buoyancy effect was still significant, reflected by the fact that the heat transfer coefficients were rather different in horizontal flow, upward flow and downward flow while other heat transfer and flow conditions were kept the same. In downward flow, the heat transfer coefficients near the pseudocritical point were much lower than those in horizontal flow, upward flow, and for constant property fluid flow. This heat transfer behavior is inconsistent with the results in the existing literature, in which heat transfer was found to be enhanced for turbulent mixed convection of variable-property fluids flowing upwards in large vertical tubes. The experimental results also indicate that the Nusselt number decreased with the reduction in tube diameter. Based on the experimental data, correlations were developed for the axially-averaged Nusselt number of forced convection heat transfer to supercritical carbon dioxide in horizontal, upward and downward flow in miniature heated tubes. The results of this study are of significance to he design of compact heat exchangers of supercritical fluids.

Acknowledgements

This work was supported by the Hong Kong Research Grant Council (RGC) Earmarked Research Grant HKUST 6046/99E.

References

[1] V.A. Kurganov, A.G. Kaptilnyi, Flow structure and turbulent transport of a supercritical pressure fluid in a vertical heated tube under the conditions of mixed condition. Experimental data, Int. J. Heat Mass Transfer 36 (13) (1993) 3383–3392.

[2] V.L. Baskov, I.V. Kuraeva, V.S. Protopopov, Heat transfer with the turbulent flow of a liquid at supercritical pressure in tubes under cooling conditions, Teplofizika Vysokikh Temperatur 15 (5) (1977) 96–102.

[3] E.A. Krasnoshchekov, I.V. Kuraeva, V.S. Protopopov, Local heat transfer of carbon dioxide at supercritical pressure under cooling conditions, Teplofizika Vysokikh Temperatur 7 (5) (1970) 922–930.

[4] S.H. Lee, J.R. Howell, Turbulent developing convective heat transfer in a tube for fluids near the critical point, Int. J. Heat Mass Transfer 41 (10) (1998) 1205–1218.

[5] N. Zhou, A. Krishnan, A. Laminar, Laminar and turbulent heat transfer in flow of supercritical CO_2, in: Proceedings of the 30th National Heat Transfer Conference, vol. 5, ASME, Portland, OR, 1995, pp. 53–63.

[6] N.E. Petrov, V.N. Popov, Heat transfer and resistance of carbon dioxide cooled in the supercritical region, Therm. Eng. 32 (3) (1985) 131–134.
[7] S. Kakac, The effect of temperature-dependent fluid properties on convective heat transfer, in: S. Kakac et al. (Eds.), Handbook of Single-phase Convective Heat Transfer, John Wiley & Sons, USA, 1987, pp. 18.1–18.56.
[8] W.B. Hall, Heat transfer near the critical point, in: J.P. Hartnett, T.F. Irvine Jr. (Eds.), Advances in Heat Transfer, vol. 7, Academic Press, USA, 1971, pp. 1–86.
[9] A.F. Polyakov, Heat transfer under supercritical pressures, in: J.P. Hartnett, T.F. Irvine Jr. (Eds.), Advances in Heat Transfer, vol. 21, Academic Press, USA, 1991, pp. 1–53.
[10] J. Pettersen, R. Rieberer, A. Leister, Heat transfer and pressure drop characteristics of supercritical carbon dioxide in microchannel tubes under cooling, in: Proceedings of 4th IIR-Gustav Lorentzen Conference on Natural Working Fluids at Purdue, 2000, pp. 99–106.
[11] S.M. Liao, T.S. Zhao, Measurements of heat transfer coefficients from supercritical carbon dioxide flowing in horizontal mini/micro channels, ASME J. Heat Transfer 124 (2) 413–420.
[12] T.M. Adams, S.I. Abdel-Khalik, S.M. Jeter, Z.H. Qureshi, An experimental investigation of single-phase forced convection in microchannels, Int. J. Heat Mass Transfer 41 (6–7) (1998) 851–857.
[13] M. McLinden, S.A. Klein, E.W. Lemmon, A.P. Peskin, NIST Thermodynamic and Transport Properties of Refrigerants and Refrigerant Mixtures—REFPROP, Version 6.01, National Institute of Standards and Technology, USA, 1998.
[14] N.B. Taylor, C.E. Kuyatt, Guidelines for Evaluating and Expressing the Uncertainty of NIST Measurement Results, NIST Technical Note 1297, National Institute of Standards and Technology, USA, 1994.
[15] J.D. Jackson, W.B. Hall, Influences of buoyancy on heat transfer to fluids flowing in vertical tubes under turbulent conditions, in: S. Kakac, D.B. Spalding (Eds.), Turbulent Forced Convection in Channels and Bundles, Hemisphere, 1979, pp. 613–640.
[16] W. Aung, Mixed convection in internal flow, in: S. Kakac, R.K. Shah, W. Aung (Eds.), Handbook of Single-phase Convective Heat Transfer, John Wiley & Sons, 1987, pp. 15.1–15.51.
[17] J.D. Jackson, W.B. Hall, J. Fewster, A. Watson, M.J. Watts, "Heat Transfer to Supercritical Pressure Fluids", U.K.A.E.A. A.E.R.E.-R 8158, Design Report 34, 1975.